

Bringing Bioelectricity to Light

Adam E. Cohen^{1,2} and Veena Venkatachalam³

¹Department of Chemistry and Chemical Biology and ²Department of Physics,

³Program in Biophysics, Harvard University, Cambridge, Massachusetts 02138;
email: cohen@chemistry.harvard.edu, veenav@gmail.com

Annu. Rev. Biophys. 2014. 43:211–32

First published online as a Review in Advance on
April 24, 2014

The *Annual Review of Biophysics* is online at
biophys.annualreviews.org

This article's doi:
10.1146/annurev-biophys-051013-022717

Copyright © 2014 by Annual Reviews.
All rights reserved

Keywords

membrane voltage, optogenetics, electrophysiology

Abstract

Any bilayer lipid membrane can support a membrane voltage. The combination of optical perturbation and optical readout of membrane voltage opens the door to studies of electrophysiology in a huge variety of systems previously inaccessible to electrode-based measurements. Yet, the application of optogenetic electrophysiology requires careful reconsideration of the fundamentals of bioelectricity. Rules of thumb appropriate for neuroscience and cardiology may not apply in systems with dramatically different sizes, lipid compositions, charge carriers, or protein machinery. Optogenetic tools are not electrodes; thus, optical and electrode-based measurements have different quirks. Here we review the fundamental aspects of bioelectricity with the aim of laying a conceptual framework for all-optical electrophysiology.

Contents

INTRODUCTION	212
WHAT GENERATES MEMBRANE VOLTAGE?	214
Membrane Voltage at Thermal Equilibrium	214
Nonequilibrium Membrane Voltages	219
WHY DOES MEMBRANE VOLTAGE MATTER?	221
PATCH CLAMP VERSUS OPTOGENETICS	223
Perturbing Membrane Voltage	223
Measuring Membrane Voltage	224
THE FUTURE OF OPTICAL ELECTROPHYSIOLOGY	226
Reporters of Absolute Voltage	227
Voltage Integrators and Voltage Samplers	227
CONCLUSION	228

INTRODUCTION

Bioelectric phenomena are ubiquitous. Lipid membranes are insulators bathed in a conducting milieu. Any lipid membrane can, in principle, support a transmembrane electric field and thus a voltage difference between its faces. The electric field tugs on charges in the membrane; these charges may be in lipid head groups, transmembrane proteins, or membrane-embedded redox molecules. Membrane voltage modulates the free-energy landscape of all molecules associated with the membrane. Any statement about the kinetics or thermodynamics of a membrane-associated process must specify the membrane voltage.

This simple fact has wondrous and far-reaching implications. The importance of membrane voltage is well appreciated in neurons and cardiomyocytes, both of which produce fast and large-amplitude electrical spikes. But the association of electrophysiology with these two cell types is also partly a consequence of how we measure membrane voltage. For electrode-based measurements the cell must be mechanically accessible, nonmotile, and large enough to impale. Patch clamp connections tend to degrade over time, so fast spikes are easier to measure than long-term shifts in baseline voltage. Many membrane-bound structures are inconvenient or impractical to measure with electrodes and thus have been little studied from an electrophysiological perspective. Examples are membrane-enveloped viruses (24), cellular organelles [mitochondria (44), nuclear membrane (53), endoplasmic reticulum (76), and the many types of intracellular vesicles], microorganisms [bacteria (21, 47, 51), yeast (32)], motile cells [sperm (45), amoeboid slime molds (60), immune cells (13)], cells with a cell wall [plants (91) and fungi (79)], and tissues undergoing morphogenesis [developing embryos (85), healing wounds (64)]. The limited experimental data available suggest that in most of these systems, voltage is dynamically regulated. Yet our ability to explore the role of voltage has, until recently, been constrained by available tools.

With the advent of new optical approaches for measuring and perturbing membrane voltage, we argue that the time has come for a renaissance in the study of bioelectricity in these “unconventional” systems. In embarking on such a study, one must reexamine the fundamental tenets of electrophysiology in the context of different physical parameters: Well-established intuitions appropriate for neuronal electrophysiology might not apply to systems with dramatically different sizes (see sidebar, Electrophysiology in Small Systems), lipid compositions, ionic environments,

ELECTROPHYSIOLOGY IN SMALL SYSTEMS

Optical voltage measurements could be applied to vesicles (endocytic or secretory), lipid-enveloped viruses, and bacteria. An indication of the surprises waiting in this domain comes from optical measurements of membrane voltage in bacteria. *Escherichia coli* expressing a proteorhodopsin-based optical voltage indicator (PROPS) showed diverse electrical spiking behaviors that responded sensitively to ionic and pharmacological perturbations (47).

However, electrophysiology in prokaryotes likely differs from that in eukaryotes. The membrane capacitance of a bacterium is between 10^{-14} and 10^{-13} F (assuming a specific capacitance of $1 \mu\text{F}/\text{cm}^2$ and typical bacterial dimensions). A single ion channel opening with a conductivity of 100 pS can alter the membrane potential with a time constant of 10^{-3} – 10^{-4} s. In contrast, neurons only fire through the concerted action of a large number of ion channels.

Additionally, because of their small volume, prokaryotes have a less robust ionic composition than do eukaryotes. A bacterium with a volume of 1 fL and a cytoplasmic Na^+ concentration of 10 mM contains only $\sim 10^7$ atoms of Na^+ . A single ion channel passing a current of 2 pA can deplete this store in less than 1 s. Finally, the number of channels of any particular type might be countably small. Stochastic insertion or degradation events or posttranslational modifications might qualitatively change the electrophysiological state of a cell. These simple estimates show that one may need to rethink many of the tenets of neuronal electrophysiology in the context of prokaryotes.

and/or protein machinery. One can expect a variety of new phenomena to arise in the context of unconventional electrophysiology.

Technical aspects of optical electrophysiology also differ from conventional patch clamp in several subtle but critically important ways. In whole-cell patch clamp, the patch pipette provides a near infinite reservoir in diffusive contact with the cytoplasm. Dialysis of cellular contents can suppress naturally occurring changes in cytoplasmic composition. In contrast, the cell membrane remains intact in optogenetic electrophysiology, so natural compositional fluctuations are preserved. In addition, current injection from the patch pipette does little to directly influence cellular composition in patch clamp electrophysiology, whereas for optogenetic currents, each ionic species must individually achieve mass balance across the cell membrane. Endogenous co-transporters and antiporters can lead to surprising couplings of the optogenetically pumped ion to fluxes of other “bystander” ions.

Patch clamp and optical electrophysiology are fundamentally different in that they measure different things: Patch clamp reports the total voltage drop across the membrane and its associated double layers, whereas optical probes sense local intramembrane electric fields. These two quantities are related but not identical. Membranes can have strong internal electric fields generated by asymmetries in ionic environment or lipid composition. These electric fields do not contribute to the membrane potential as measured by patch clamp, but they can strongly influence membrane permeability and the conformations of transmembrane proteins. One must remember that the electrostatic potential profile across the membrane cannot be described by a single number; patch clamp and optical techniques report different aspects of the complex potential profile.

In this review, we address three questions: What generates membrane voltage? How does membrane voltage affect processes in the membrane? What are the challenges and opportunities of optical versus electrode-based electrophysiology? As the literature on electrical measurements in unconventional systems spans more than a century and is too vast and scattered to review in depth, we instead highlight a few measurements that illustrate important biophysical principles. Some of this material is discussed in older literature and textbooks (41, 55), but it merits reexamination

in light of improved technology. Our primary purpose is to encourage the reader to contemplate the role of membrane voltage in her or his favorite system.

WHAT GENERATES MEMBRANE VOLTAGE?

Membranes can contain diverse ion channels, exchangers, pumps, and redox molecules. How does one calculate the membrane voltage? Or, of more concern to the experimentalist, what do measurements of membrane voltage and its susceptibility to ionic and pharmacological perturbations teach us about the transporters in the membrane? The Nernst and Goldman equations as typically taught in introductory neurobiology classes encompass only a limited subset of biologically important scenarios. To understand the full diversity of bioelectric phenomena, we must return to the basics.

To illustrate the need for a more general approach, let us consider the mitochondrial membrane potential, which has been indirectly inferred to be in the range of -150 to -190 mV (63, 68). None of the major ions in mitochondria (H^+ , K^+ , Na^+ , Ca^{2+}) has a concentration gradient strong enough to generate a Nernst potential of -150 mV. Application of the Goldman equation does not help because the Goldman equation always predicts a membrane voltage that lies between the Nernst potentials of the individual ions. Furthermore, mitochondria contain ion pumps, ion exchangers, redox couples, and metabolite carriers (68). The associated charge fluxes clearly contribute to the membrane voltage, but the Nernst and Goldman equations as usually written do not accommodate these types of electric currents.

Tables 1 and 2 show seven physical processes that can generate a membrane voltage, several of which are often at play simultaneously. We classify these processes into those that occur at thermal equilibrium and those that require a nonequilibrium steady state. Membrane voltages at thermal equilibrium can persist indefinitely, even in the absence of metabolic input (except for the gradual dissipation of ion concentration gradients resulting from leakage through the membrane). In the nonequilibrium scenarios, active ion pumps or exchangers are needed to maintain the concentration gradients that lead to the voltage. For a lucid discussion of some of these mechanisms, the reader is referred to Reference 41.

Membrane Voltage at Thermal Equilibrium

Consider an arbitrary charge-transfer process across a membrane. For the moment, let us restrict our discussion to a single concerted reaction for which membrane voltage influences the reaction rate. Thermal equilibrium occurs when the voltage is such that the forward and reverse rates are equal. The net transport of charge across the membrane is then zero, and the net transport of each species is also zero. Basic thermodynamics tells us that the membrane potential at thermal equilibrium is

$$V^{\text{in-out}} = V_0 + \frac{RT}{zF} \ln Q, \quad 1.$$

where V_0 is the membrane potential that would exist if all species were in their standard states (1 M activity, 25°C), z is the number of positive charges transferred from the inside to the outside per reaction cycle, F is the Faraday constant (the electric charge of one mole of protons), and Q is the reaction quotient (product concentrations raised to their stoichiometric coefficients and multiplied, divided by reactant concentrations, raised to their stoichiometric coefficients and multiplied). (In the electrochemistry literature, the sign on the second term is reversed because one is usually dealing with electrons; here we consider positively charged ions.) At room temperature (22°C) and $z = 1$, Equation 1 implies a decrease in V of 58.6 mV for every tenfold decrease in Q .

Table 1 Membrane voltages at thermal equilibrium

Physical scenario	Schematic	Examples
Single permeable ion		Approximate resting potential in neurons and T lymphocytes (13, 12)
Coupled transport of multiple ions; coupled transport of ions and metabolites		ClC chloride/proton antiporters (1), NhaA sodium/proton antiporter (86), NCX sodium/calcium antiporter (6)
Coupled transport of ions and a chemical reaction		F ₀ F ₁ ATPase (62), Na ⁺ /K ⁺ ATPase
Redox reaction		Oxidative phosphorylation in bacteria, mitochondria, and chloroplasts (62); oxidative burst in phagocytes (4, 20, 77) and some plant plasma membranes (72)
Donnan potential: single impermeable ion		Vertebrate skeletal muscle (36), erythrocytes (26, 37), nuclear envelope (53), some viral capsids (88), and cartilage (50)

Any chemical transformation that transports charge across a membrane reaches thermal equilibrium when the thermodynamic driving force of the reaction balances the change in electrostatic energy of the transported charge. The driving force can come from diffusion, chemical reactions, or redox reactions. Each reaction scheme is described in detail in the main text.

Although Equation 1 is familiar to any student of introductory electrochemistry, its implications for bioelectricity are often underappreciated.

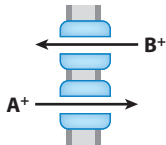
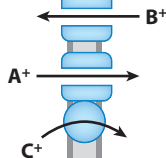
Nernst. In the simplest case, a membrane is solely permeable to a single ion. For instance, the reaction could be $K_{in}^+ \leftrightarrow K_{out}^+$ via the $K_v1.3$ voltage-gated potassium channel found in human T lymphocytes (13, 12). Here $z = 1$. There are no chemical transformations, so $V_0 = 0$. Equation 1 then reduces to the Nernst equation as usually written in neuroscience textbooks:

$$V^{in-out} = \frac{RT}{zF} \ln \frac{C_{out}}{C_{in}}. \quad 2.$$

Thermal equilibrium is reached when the electrostatic driving force is just strong enough to counteract the tendency of K^+ ions to diffuse from a high concentration to a low concentration.

Coupled transport. Symporters and antiporters couple transport of multiple species with a well-defined stoichiometry and sometimes with a net transport of charge. Examples include the mammalian chloride transporters ClC-4, ClC-5, and ClC-7 (30, 66) and their bacterial homolog,

Table 2 Nonequilibrium membrane voltages

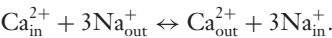
Physical scenario	Schematic	Examples
Goldman–Hodgkin–Katz: multiple permeable ions, independent transport of each		Neurons, cardiomyocytes, Purkinje fibers
Goldman with a current source: electrogenic pump		H ⁺ pump: mitochondria (59), <i>Escherichia coli</i> (23), <i>Neurospora crassa</i> (74)
		Na ⁺ pump: neutrophils (3), mast cells (9)
		Cl [−] pump: epithelial membranes (27), some plant cells (<i>Acetabularia mediterranea</i>) (73)

At the steady state, the net flux of charge is zero, and the net flux of each ion is also zero. The steady-state voltage depends on the i - V relationship of each charge transporter, which in turn depends on the detailed molecular mechanism. For each species, the route into the cell may differ from the route out of it, so detailed balance is not preserved. These voltages require a continuous input of energy. Each reaction scheme is described in detail in the main text.

CLC-ec1 (1). These proteins couple H⁺ export with Cl[−] import, resulting in a net export of two charge units. The mammalian CLC antiporters reside in intracellular acidifying membranes, whereas CLC-ec1 regulates response to extreme acidity in *Escherichia coli* (40).

Many other electrogenic transporters have been characterized in detail. The *E. coli* antiporter NhaA exchanges two H⁺ ions for one Na⁺ ion and is important for maintaining a low intracellular sodium concentration in this species (86). Mammalian sodium-calcium exchangers (NCX) couple the export of one Ca²⁺ ion with the import of three Na⁺ ions; these transporters are important in maintaining low basal concentrations of Ca²⁺ in neurons and cardiomyocytes (6). Mitochondria have several electrogenic inner membrane cotransporters: the ATP/ADP exchanger (adenine nucleotide translocator, ANT), the aspartate/glutamate carrier (AGC), and the mitochondrial sodium/calcium exchanger (NCLX) (68). Mitochondria also contain electrogenic transporters of single ions: the calcium uniporter (MCU) and the proton-conducting uncoupling proteins (UCP).

How does one calculate equilibrium membrane voltage for an electrogenic exchanger? Which way will the exchanger run for a specified membrane voltage and set of ion concentrations? Let us consider the example of the NCX. The reaction is



The net charge transfer is $z = -1$ (one positive charge is imported), and there are no chemical transformations or redox reactions, so $V_0 = 0$. Thus, the reaction quotient is as follows:

$$Q = \frac{[\text{Na}_{\text{in}}^{+}]^3 [\text{Ca}_{\text{out}}^{2+}]}{[\text{Na}_{\text{out}}^{+}]^3 [\text{Ca}_{\text{in}}^{2+}]}.$$

One can split the term $\ln Q$ in Equation 1 into a sodium-dependent part and a calcium-dependent part, each of which contains the expression for the Nernst potential of only that ion. Thus, $V^{\text{in-out}} = (3V_{\text{Na}^{+}} - 2V_{\text{Ca}^{2+}})$, where $V_{\text{Na}^{+}}$ and $V_{\text{Ca}^{2+}}$ are the Nernst potentials of the sodium and calcium ions, respectively. Note that this formula differs from the Goldman equation discussed below, which corresponds to a nonequilibrium situation with independent transport of multiple ions.

Electroneutral exchangers ($z = 0$) cannot support an equilibrium membrane voltage on their own. For instance, the mammalian Na-K-Cl cotransporters NKCC1 and NKCC2 import Na⁺,

K⁺, and Cl⁻ in a 1:1:2 stoichiometry and thus transport no net charge (33). However, by modifying the current–voltage relations of the individual ions, these exchangers can influence nonequilibrium voltages (see below). The NKCC cotransporters are found in many mammalian tissues, in which they play an important role in regulating osmotic balance. Many of the mitochondrial transporters are also electroneutral. For example, the P_i/H⁺ carrier (P_iC) catalyzes the following reaction: $\text{H}_2\text{PO}_4^-_{\text{out}} + \text{H}^+_{\text{out}} \leftrightarrow \text{H}_2\text{PO}_4^-_{\text{in}} + \text{H}^+_{\text{in}}$ (82).

Redox. Transmembrane electron transfer is well known as a critical aspect of metabolism. Mitochondria and prokaryotes use transmembrane redox reactions to convert chemical energy into a membrane voltage, which in turn provides part of the proton-motive force that powers the ATP synthase. Chloroplasts use solar energy to achieve a similar outcome. Yet transmembrane redox processes have also been detected in plasma membranes and intracellular organelles, often playing unanticipated roles. We speculate that redox reactions in membranes are more widespread than is currently thought.

Cells use plasma membrane electron transport (PMET) to maintain redox homeostasis (in some plant cells), defend against pathogens (in immune cells), and regulate growth (19). For a review of PMET in mammalian cells, the reader is referred to Reference 69. The best-documented example of mammalian PMET occurs in phagocytes, in which a nicotinamide adenine dinucleotide phosphate (NADPH) oxidase mediates transmembrane electron transfer to form superoxide, which kills pathogens (4, 71). The reaction is as follows:



This reaction is electrogenic and has been measured to have an equilibrium potential of $V \approx +190$ mV (20). Here, $z = -2$ (two electrons exit the cell).

The thermodynamic analysis of transmembrane electron transfer begins, again, with Equation 1. The key new feature is that electrons do not exist in free solution, only bound in molecules. Thus there can be an energy difference associated with a change in the quantum state of the electron between reactants and products. This fact introduces a nonzero value for V_0 in Equation 1. The standard reduction potential for $\text{NADP}^+ + \text{H}^+ + 2\text{e}^- \rightarrow \text{NADPH}$ is -320 mV (using the biochemical standard state of pH 7) (11), and the standard reduction potential for $\text{O}_2 + \text{e}^- \rightarrow \text{O}_2^-$ is $+160$ mV (at $[\text{O}_2] = 1$ M) (94). Thus, the standard cell potential, V_0 , is equal to $+160$ mV. The equilibrium membrane voltage is given by the following equation:

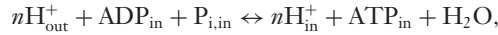
$$V^{\text{in-out}} = V_0 - \frac{RT}{2F} \ln \frac{[\text{O}_{2,\text{out}}^-]^2 [\text{NADP}^+_{\text{in}}]}{[\text{O}_{2,\text{out}}]^2 [\text{NADPH}_{\text{in}}]}.$$

Inside the cell, $[\text{NADPH}] \gg [\text{NADP}^+]$, whereas outside the cell, $[\text{O}_2] \gg [\text{O}_2^-]$. Both factors drive the equilibrium voltage more positive than its standard state value.

Electron transport across the plasma membrane has also been reported in liver cells (90), erythrocytes (84), insulin-secreting pancreatic beta cells (31), and the plasma membranes of some plants (thoroughly reviewed in 72). Transmembrane electron transport also occurs in subcellular compartments. For instance, cytochrome b561 mediates electron transfer across catecholamine secretory vesicles for the purpose of reducing dopamine to noradrenaline (81). To our knowledge, it is not known whether PMET occurs in canonically active cells such as neurons and cardiomyocytes, or whether glia use it for maintaining redox homeostasis in the brain.

Ion transfer coupled to a chemical reaction. Ion transfer coupled to a chemical reaction that does not involve transmembrane electron transport requires a slightly different analysis. The paradigmatic example is the F₀F₁ ATPase, which imports 8 to 14 protons and synthesizes three

molecules of ATP from ADP and P_i in the process (62). What determines whether the F_0F_1 ATP synthase consumes ATP and exports protons or generates ATP and imports protons? The reaction involved is as follows:



where n is typically between 3 and 4. For simplicity, let us assume $n = 4$, in which case $z = -4$. V_0 is determined by the synthesis of ATP, from the equation $V_0^{ATP} = \frac{\Delta_r G_0}{zF}$, where $\Delta_r G_0 = 30.5$ kJ/mol is the standard free energy of reaction for $ADP + P_i \rightarrow ATP$ (note that this quantity depends on the concentration of Mg^{2+} and the pH). Thus $V_0^{ATP} \approx -80$ mV. The reaction quotient is

$$Q = \frac{[H_{in}^+]^n [ATP_{in}]}{[H_{out}^+]^n [ADP_{in}] [P_{i,in}]}.$$

This expression simplifies upon expanding the logarithm to obtain the following equation:

$$V_{eq}^{in-out} = V_0^{ATP} + 59 \text{ mV} \times \Delta pH^{in-out} - \frac{59}{n} \text{ mV} \times \log Q_{ATP}^{synth}.$$

The pH gradient ranges from 0.5 to 1.2 pH units (the mitochondrial lumen being more basic), thus the second term has a value of 30 to 70 mV (68). The concentrations of ATP, ADP, and P_i can vary with metabolic state, but typically, the ratio of mitochondrial $[ATP]:[ADP] \approx 2$, and $[P_i] \approx 70$ mM (56, 78), yielding $\log Q_{ATP}^{synth} \approx 1.5$. Combining these values, $V_{eq}^{in-out} \approx -70$ mV. For $V < V_{eq}$, the F_0F_1 ATP synthase imports protons and produces ATP; for $V > V_{eq}$, the enzyme exports protons and consumes ATP. As one would hope, the measured membrane voltages imply that mitochondria usually produce ATP.

A similar analysis can be applied to the Na^+/K^+ ATPase, which maintains the sodium and potassium concentration gradients needed to sustain electrical activity in neurons and cardiomyocytes. The reaction for this protein is



As with the ATP synthase, we can estimate how close to thermal equilibrium this enzyme typically operates. Here, $z = 1$, so $V_0^{ATP} \approx -320$ mV. The reversal potential is

$$V_{eq}^{in-out} = V_0^{ATP} + 59 \text{ mV} \times \log Q_{ATP}^{hydr} + 3V_{Na} - 2V_{K}.$$

For the hydrolysis of ATP, $\log Q_{ATP}^{hydr} \approx -2.5$ to -3 at cytoplasmic concentrations ($[ATP]:[ADP] \approx 5$ – 10 , $[P_i] \approx 10$ mM; see Reference 78). In a mammalian neuron, we have $V_{Na} = 56$ mV and $V_{K} = -102$ mV. Combining these numbers yields $V_{eq}^{in-out} = -95$ to -125 mV. For $V > V_{eq}$, the Na^+/K^+ ATPase hydrolyzes ATP, pumps Na^+ ions out of the cell, and pumps K^+ ions into the cell; for $V < V_{eq}$, the enzyme uses ion concentration gradients to synthesize ATP. Neurons typically have a resting potential near -70 mV. If the resting potential were too close to the reversal potential, then this reaction would proceed too slowly to compensate for the slight Na^+ influx and K^+ efflux of that accompany each action potential.

The membrane potentials with the largest magnitude are found in some plants and fungi, in which the voltage can approach -300 mV (74). Our thermodynamic analysis above shows that the Na^+/K^+ ATPase cannot possibly be responsible for this voltage. Rather, these extreme voltages largely result from the activity of electrogenic ATP-powered proton pumps, which drive the reaction $H_{in}^+ + ATP_{in} \leftrightarrow H_{out}^+ + ADP_{in} + P_{i,in}$ (80). Thermodynamic considerations provide a firm bound on the membrane voltage. Under basal physiological conditions (not the thermodynamic standard state), the free energy of ATP hydrolysis is $\Delta_r G \approx -45$ kJ/mol. The greatest voltage is obtained for export of a monovalent ion, i.e., when $z = 1$. The pH difference across the membrane

is small, so $V_{\max} \approx -460$ mV. Because their membrane voltages are large, the first quantitative measures of bioelectrical phenomena were obtained from the leaves of the Venus flytrap, *Dionaea muscipula*, in 1872 (75). Action potentials were later discovered in the aquatic plant *Nitella* and measured using extracellular electrodes (38).

Donnan. In some cells, the membrane is permeable to all ions except one, often a large polyanion such as DNA or RNA. This situation applies to the nuclear envelope (53), vertebrate skeletal muscle (36), and possibly viral capsids (88). Entropy favors a uniform distribution of the mobile ions, but electrostatics requires an excess of mobile cations inside the membrane to offset the charge of the impermeable polyanions. The competition between entropy and electrostatics leads to a membrane voltage.

Let us consider the simple case of a polyanion, N^{-w} , with a charge of $-w$, and a simple salt, KCl, where both the K^+ ions and the Cl^- ions can freely permeate the membrane. Each permeable ion achieves a concentration ratio given by the Nernst equation (Equation 2):

$$V = \frac{RT}{F} \ln \frac{[K_{\text{out}}^+]}{[K_{\text{in}}^+]} = -\frac{RT}{F} \ln \frac{[Cl_{\text{out}}^-]}{[Cl_{\text{in}}^-]}. \quad 3.$$

We further require overall charge neutrality in the region with the polyanion, so

$$[Cl_{\text{in}}^-] + w[N_{\text{in}}^{-w}] = [K_{\text{in}}^+]. \quad 4.$$

Finally, the concentrations on the outside are usually clamped by connection to a large reservoir: $[Cl_{\text{out}}^-] = [K_{\text{out}}^+] = C_0$. One can then solve for $[Cl_{\text{in}}^-]$, $[K_{\text{in}}^+]$, and V to find

$$V^{\text{in-out}} = -\frac{RT}{F} \ln \left(\frac{w[N^{-w}]}{2C_0} + \sqrt{\left(\frac{w[N^{-w}]}{2C_0} \right)^2 + 1} \right). \quad 5.$$

As an example, we estimate the Donnan potential of the human nuclear envelope. We approximate the nucleus as a sphere with a diameter of 6 μm . Each of the 6×10^9 base pairs in a diploid cell has two anionic phosphate groups, so the concentration of these anions is approximately 200 mM. The ionic strength of cytoplasm, which determines the concentration of mobile charges, is similar; $C_0 \approx 150$ mM. If DNA were the only membrane-impermeable species, then the Donnan potential of the nuclear envelope would be approximately -36 mV. However, DNA is wrapped with positively charged histones, which significantly decrease the mean charge density in the nucleus. Measurements of the nuclear membrane potential give a value of approximately -15 mV (48, 53). The possibility of a Donnan potential in viral capsids has been considered theoretically, but this potential has never been measured experimentally (88).

Donnan potentials can also arise in the absence of a membrane. Simply having a cross-linked ionic hydrogel, such as cartilage, is sufficient. At physiological pH, the proteins that make up cartilage are predominantly negatively charged and have a charge density of approximately 200 mM (50). Thus, at physiological ionic strength ($C_0 \approx 150$ mM), the Donnan potential of cartilage is approximately -36 mV. As the ionic strength of the solution decreases, its Donnan potential increases.

Nonequilibrium Membrane Voltages

We have now discussed several diverse sources of membrane voltage at thermal equilibrium. But, equilibrium is death; most biologically interesting systems are far from equilibrium. To create a nonequilibrium situation, one need only establish in the same membrane two independent

membrane transport processes that have different equilibrium voltages. One process will speed up and the other will slow down until they reach a nonequilibrium steady state at an intermediate voltage that requires continuous energy input to maintain.

We were able to calculate equilibrium membrane voltages on the basis of thermodynamic principles alone, without accounting for the microscopic details of the charge transport processes. For the nonequilibrium systems, however, we are not so lucky. Analyses of these systems require microscopic models of their dynamics and are therefore, by necessity, approximate.

Goldman. When a membrane is permeable to more than one ion, each ion can have a nonzero transmembrane flux, provided that the net electric current summed over all ions is zero. Mass balance for each ion is achieved by invoking active transporters that counteract the passive flux but that do not otherwise appear in the analysis. If one knows how the current for each species varies as the voltage deviates from the equilibrium value for that species, then one can find the voltage at which the net current is zero.

In the most trivial nonequilibrium model, one might assume that the current for each ion grows linearly as the voltage deviates from its equilibrium value, i.e., $i_j = \sigma_j(V - V_j)$, where σ_j is the conductance for species j and V_j is its Nernst potential. The requirement of no net current is as follows: $\sum_j i_j = 0$. In this model, the steady state voltage is simply a weighted average of the Nernst potentials of each ion, just as we found for the case of concerted cotransport:

$$V_{\text{lin}} = \frac{\sum_j \sigma_j V_j}{\sum_j \sigma_j}.$$

It is an experimental fact that many ion channels show asymmetric current–voltage relations with greater apparent conductivity when the current draws ions from the side of the membrane with higher concentration. This asymmetry is often referred to as rectification. Goldman, Hodgkin, and Katz created a simple model for nonequilibrium ionic transport that reproduces this rectification behavior. The derivation is given in many textbooks (e.g., 41) and is therefore not repeated here. For a voltage dominated by monovalent ions, the Goldman–Hodgkin–Katz equation for the steady-state voltage is

$$V = \frac{RT}{F} \ln \frac{\sum_i \mu_i [M_i^+]_{\text{out}} + \sum_j \mu_j [M_j^-]_{\text{in}}}{\sum_i \mu_i [M_i^+]_{\text{in}} + \sum_j \mu_j [M_j^-]_{\text{out}}}, \quad 6.$$

where μ_i is the ionic permeability for species i . To preserve the steady-state ionic concentrations, we invoke a metabolically powered pump or exchanger. In neurons, this exchanger is predominantly the Na^+/K^+ ATPase, but the Goldman analysis ignores the electrogenic nature of the Na^+/K^+ ATPase.

The impact of optogenetically actuated ion channels (e.g., channelrhodopsins) on membrane voltage can be understood in the context of the Goldman equation. Illumination of channelrhodopsin introduces an additional conductance. The impact of this conductance on voltage depends on both intracellular and extracellular ionic conditions, as well as the other endogenous membrane conductances. Depending upon the capacities of endogenous pumps and ion-exchange mechanisms, steady-state activation of a large optogenetic current may also significantly perturb intracellular ion concentrations.

Goldman with a pump. We have seen that when electrogenic charge transport is coupled to a chemical reaction, the V_0 term in Equation 1 can be significantly larger than the concentration-dependent term. In this case, the equilibrium membrane potential can exceed the diffusion potential of any ion (Equation 2). One often finds an electrogenic chemical reaction occurring in parallel

with several diffusive charge-transport processes. The voltage in this scenario can be estimated from a revision of the Goldman equation to include a current source.

In the presence of a pump, the sum of the passive electric currents is not zero, but rather $\sum_j i_j = -i_{\text{pump}}$. If one assumes the same ion channel model that led to the Goldman equation, then the membrane voltage in the presence of a current source is

$$V = \frac{RT}{F} \ln \frac{\sum_i \mu_i [M_i^+]_{\text{out}} + \sum_j \mu_j [M_j^-]_{\text{in}} + J_{\text{pump}}}{\sum_i \mu_i [M_i^+]_{\text{in}} + \sum_j \mu_j [M_j^-]_{\text{out}}}, \quad 7.$$

where J_{pump} is the current density of the current source. Of course, if J_{pump} is produced by a chemically or optically powered protein (as opposed to a patch pipette) then J_{pump} depends on V . There will exist a so-called stall voltage, at which the value of J_{pump} goes to zero. However, when the pump is operated far from equilibrium, the voltage dependence of J_{pump} can often be ignored.

Together, electrogenic pumps and passive diffusion determine the membrane voltage in mitochondria ($V = -150$ mV to -190 mV) (63, 68), *E. coli* ($V = -140$ mV to -80 mV) (23), neutrophils (3), and mast cells (9). In mitochondria and *E. coli*, oxidative phosphorylation produces an electrogenic proton current, whereas in mammalian plasma membranes, the most significant electrogenic pump is typically the Na^+/K^+ ATPase (which pumps 3 Na^+ ions out of the cell and pumps 2 K^+ into it). Equation 7 can also be used to model membrane voltage when the electrogenic pump is powered by a photochemical reaction, as occurs in chloroplasts and in membranes containing microbial rhodopsin charge pumps (e.g., halorhodopsin, archaerhodopsin).

WHY DOES MEMBRANE VOLTAGE MATTER?

Membrane voltage influences every membrane process that involves charge movement. **Figure 1** illustrates some examples. In each case, the ratio of the population on the left to the population on the right is given by a Boltzmann distribution:

$$\frac{C_L}{C_R} \propto e^{-\frac{qV}{k_B T}}, \quad 8.$$

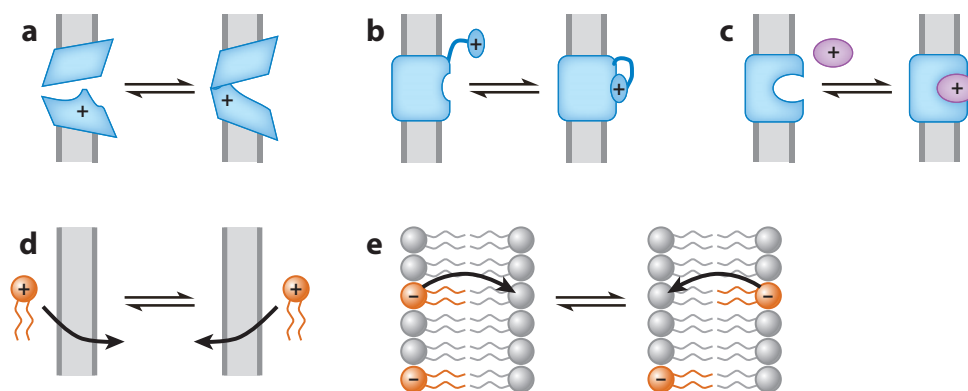


Figure 1

Mechanisms by which membrane voltage can influence membrane-associated processes. (a) Voltage gating of ion channels is well known, but voltage can also affect (b) conformations of proteins other than ion channels, (c) binding of charged ligands, (d) concentrations of charged amphiphiles, and (e) distributions of charged species within the membrane.

where q is the amount of charge that moves between the two states, V is the voltage difference through which the charge moves, k_B is Boltzmann's constant, and T is the absolute temperature.

The best-known example of voltage regulation is the gating of voltage-dependent ion channels (**Figure 1a**). These channels are famous for their role in neurons, but bacteria also contain sodium channels, inward-rectifier potassium channels, and voltage-gated potassium channels (7, 25), although their biological functions are largely unknown (52). Ion channels have been comparatively easy to characterize because a voltage-induced conformational change results in a change in the ionic current that can be directly measured with an electrode.

However, the role of voltage goes further. Every membrane-bound enzyme, receptor, or transporter experiences conformational stresses as a result of membrane voltage pulling on its charged amino acids. If the protein has multiple conformational states, the balance between these states is given by Equation 8. Thus, voltage may regulate the activity of the protein, but conventional electrode-based measurements may be unable to detect its influence (**Figure 1b**). The best-known example of this phenomenon is the voltage-sensitive phosphatase from *Ciona intestinalis*, Ci-VSP (61). The voltage-dependent activity of this protein was only demonstrated by coupling its enzymatic activity to the activation of other ion channels. Unfortunately, this trick does not generalize, so the challenge of identifying cryptic voltage-sensitive transmembrane proteins remains unsolved. However, the default assumption should be that any transmembrane protein is affected by membrane voltage; the only question is about the size of the effect for physiological voltage swings.

Membrane voltage can also strongly influence binding interactions in proteins with ligand or ion binding sites within the membrane (**Figure 1c**). For instance, changes in membrane voltage can tune the acid-base equilibria of titratable groups on the inner segments of transmembrane proteins. This fact is the basis for microbial rhodopsin-based voltage indicators, which undergo large voltage-dependent shifts in absorption and fluorescence properties (46, 47, 49). These shifts have been explained by electrical regulation of the acid-base equilibrium of a Schiff base in the protein core. Multiply charged ligands can be even more sensitive to membrane voltage. Binding of ATP in the family of ATP binding cassette (ABC) transporters is not likely to be sensitive to membrane voltage because the ATP-binding domains of these proteins are well outside the membrane. But ligand binding in G protein-coupled receptors (GPCRs) often happens deep in the protein (29) and thus is plausibly susceptible to membrane voltage.

Membrane voltage regulates transport of membrane-permeable charged species, even in the absence of specific protein transporters (**Figure 1d**). Researchers have speculated that most cells have a negative membrane voltage to facilitate accumulation and retention of amino acids (34). Bacteria are exposed to a wide range of charged amphiphiles, including bile salts and fatty acids in the intestine, as well as to many drugs and antibiotics. The negative membrane voltage causes cationic amphiphiles to accumulate in the cytoplasm. Mitochondria also act as concentrators of cationic amphiphiles on account of the strongly negative mitochondrial inner membrane voltage. The equilibrium ratio of intracellular to extracellular concentrations is given by Equation 8. Membrane voltage can also influence the distribution of charged amphiphiles within the membrane, e.g., by causing lipids to redistribute in a potential-dependent way (**Figure 1e**).

For a membrane voltage of -120 to -180 mV, the equilibrium concentration of cationic species is 100–1,000-fold higher inside the cell than outside it. This fact presents a serious challenge for bacteria: To prevent buildup of toxic cationic compounds, bacteria have evolved a range of cationic export machinery. *E. coli* contain seven distinct efflux systems to combat cationic accumulation (83). Negative membrane voltages present an energetic barrier to efflux of cationic contaminants. One plausible explanation for the electrical spiking observed in *E. coli* is that spikes temporarily remove this electrostatic barrier, facilitating rapid cation efflux. Indeed, pulsatile efflux of a cationic dye was observed to accompany spikes in bacterial membrane potential (47).

Thus, bacteria may time-share their membrane voltage to accomplish tasks requiring different directions of transmembrane charge transport.

Finally, there is evidence that membrane voltage couples directly to the mechanical properties of the membrane, particularly its bending modulus. Theoretical analyses have shown that the bending energy of a membrane increases with its surface charge density (92, 93). Remarkably, the outer hair cells involved in hearing show a bidirectional electromechanical coupling: Not only does deflection induce a voltage, but changes in membrane voltage also directly induce motion in these cells (10). Atomic force microscopy (AFM) experiments have also observed small motions associated with synaptic activation; these motions were attributed to changes in osmotic pressure accompanying activity-induced changes in ionic strength (43). Some researchers have also suggested that vesicle-fusion (100) and endocytosis (99) processes may be influenced by membrane voltage directly through a calcium-independent mechanism.

PATCH CLAMP VERSUS OPTOGENETICS

Optogenetic techniques are now widely used to perturb and to measure membrane voltage in cells. Light-gated sodium and calcium channels (channelrhodopsins and their variants) can depolarize a cell and induce firing (8). Light-driven pumps [e.g., halorhodopsins (28) and archaerhodopsins (16)] can hyperpolarize a cell and suppress firing. A palette of genetically encoded voltage indicators can report the response of cells to natural or induced stimuli (2, 65). One may think of actuators exposed to brief flashes of light with the primary intent of changing neuronal (or cardiac) firing as being roughly equivalent to a patch electrode. Moreover, indicators that are used to count spikes or to measure action potential waveforms are also roughly equivalent to a patch electrode. However, for biophysical studies, there are subtle but important differences between electrode-based and optical electrophysiology.

Perturbing Membrane Voltage

Whole-cell patch clamp fixes the intracellular concentrations of all ions and small molecules at the concentrations contained in the patch pipette filling solution. To estimate the time required for cytoplasmic components to equilibrate with a pipette, consider diffusion of a typical small molecule with a diffusion coefficient $D = 200 \mu\text{m}^2/\text{s}$. To diffuse across a cell body with diameter $d = 20 \mu\text{m}$ requires a time $t_D \approx d^2/2D = 1 \text{ s}$. This crude estimate is modified somewhat by the fact that the patch orifice is small compared with the size of the cell, but the d^2/D scaling is robust. Thus, if one is studying the response of a neuron to an extended period of activity or to pharmacological perturbations, dialysis of intracellular contents can perturb the results. These perturbations can be particularly significant for long-term measurements or for measurements on small structures. Indeed, after making a patch clamp connection to a cell, it is quite difficult to remove the pipette while keeping the cell alive and to return to the cell on a subsequent day. Cell-attached and perforated patch clamp measurements perturb intracellular contents less than do other techniques, but these techniques are technically demanding and have poorer quality of electrical access.

In contrast, optogenetic approaches preserve the integrity of the cell membrane and thereby maintain endogenous small-molecule and ion dynamics. In their inactive state, optogenetic actuators do not perturb the cytoplasmic content. But when active, these proteins can perturb ionic concentrations in ways that patch clamp does not. An optogenetic actuator injects ions of a type determined by the protein's ionic selectivity, whereas a patch pipette injects ions determined by the composition of the filling solution. Simply matching steady-state currents does not make optogenetic actuators and patch clamp equivalent. Optogenetically pumped ions can reach a steady

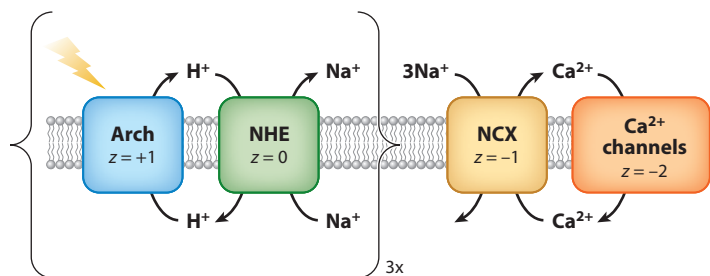


Figure 2

Coupled ion-transport processes interact with optogenetic perturbations. This example shows a series of coupled processes necessary to achieve mass and charge balance for actuation of a light-gated proton pump. Abbreviations: Arch, Archaerhodopsin 3; NCX, $\text{Na}^+/\text{Ca}^{2+}$ electrogenic exchanger; NHE, Na^+/H^+ exchanger.

state only by returning to their compartment of origin through another channel or transporter. For example, a light-driven inward chloride pump, halorhodopsin (eNpHR), has been shown to increase local chloride concentrations sufficiently to change the ion's equilibrium potential. This change shifted the reversal potential of γ -aminobutyric acid (GABA) channels (70).

The effects of other optogenetic actuators can be more subtle. We take as an example Archaerhodopsin 3 (Arch), which generates an outward membrane current, $j_{\text{pump}} \approx 10 \text{ pA/pF}$, that is nearly insensitive to membrane voltage over the physiological range (16). Under steady-state conditions, this outward current must be balanced by an equal inward proton current. The change in cytoplasmic pH depends on the native permeability of the membrane to protons: If the membrane is highly permeable, the change in pH will be small. Consistent with a large basal proton permeability, Arch-induced changes in pH have been reported to be small (16).

This phenomenon, however, is not the end of the story. Because mammalian neurons transport protons primarily via the Na^+/H^+ exchanger (NHE) (98), protons returning to the cell cause Na^+ to exit. Furthermore, Na^+ efflux is offset by means of the $\text{Na}^+/\text{Ca}^{2+}$ electrogenic exchanger (NCX). Finally, Ca^{2+} mass balance is achieved through endogenous calcium channels. **Figure 2** shows a plausible set of coupled transport processes that achieve charge and mass balance for each species. This example shows that one must carefully consider downstream ionic perturbations induced by an optogenetic actuator.

Measuring Membrane Voltage

Optical tools are now also being developed to measure membrane voltage. Significant recent advances have been made in the development of genetically encoded voltage indicators (14, 42, 46) and voltage-sensitive dyes (58, 96). However, one must exercise caution in interpreting data from these optical tools as though they were patch clamp measurements: Different tools have different quirks.

Optical measurements perturb cytoplasmic composition less than do electrical measurements. However, phototoxicity can be a concern, as can the displacement or disruption of endogenous ion channels by the reporters. Every optical voltage sensor must contain some charge that moves in response to changes in membrane voltage. This mobile charge contributes to increased membrane capacitance, which can distort or even suppress action potential waveforms. Capacitive loading is small in rhodopsin-based protein indicators (49) and molecular wire-based organic dyes (58) but is significant in some hybrid protein/small molecule voltage sensors (15).

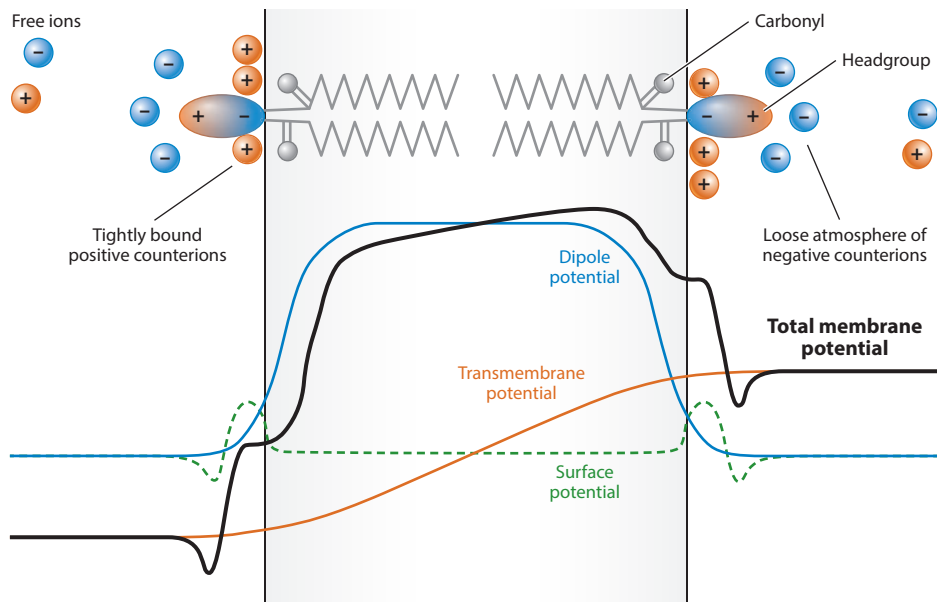


Figure 3

Contributions to the electrical potential profile in a membrane. Charged and dipolar lipid headgroups create a surface potential and a dipole potential, respectively. If either of these quantities is asymmetric across the lipid bilayer, then an electric field may permeate the membrane. This internally generated electric field is undetectable by conventional patch clamp and does not affect equilibrium ionic distributions in the bulk. However, it does act on the conformations of transmembrane proteins and regulates membrane permeability. Adapted with permission from Reference 22.

A more fundamental difference between optical and patch clamp measurements is that they report different physical parameters. Optical indicators sense the local electric field in the membrane, whereas patch clamp measurements report the full voltage drop across the membrane and the surrounding electrical double layers. These two quantities can differ for several reasons.

Close examination of a lipid membrane shows that the electric field is not homogeneous across the membrane. Indeed, many factors besides the membrane potential contribute to the intramembrane electric field: The contributions of these factors explain how the activation thresholds of voltage-gated ion channels could depend on the lipid or ionic environment. For excellent reviews of the potential profiles in lipid membranes, the reader is referred to References 17, 54, and 55. **Figure 3** shows a typical electrical potential profile across a lipid membrane. Let us consider the contributions to this profile one at a time.

Surface potential. The surface potential arises from a balance between the tendency of ionizable lipid headgroups to dissociate and the resulting electrostatic attraction between the charged headgroups and their counterions in solution. Most biological membranes contain a mixture of anionic and zwitterionic lipids. For example, the surface potential of a typical mammalian plasma membrane that contains 20% anionic lipids and has an area per lipid headgroup of 60 \AA^2 in a 0.1 M salt solution is approximately -60 mV relative to the bulk liquid (55). The biological implications of this surface potential are discussed in Reference 54.

An asymmetry in the surface potential on opposite sides of a membrane leads to a transmembrane electric field, even in the complete absence of a macroscopically measurable membrane

potential. This asymmetry can arise either from differences in the density of anionic lipid headgroups or from differences in the ionic composition of the solutions on opposite sides of the membrane. Monovalent ions (Na^+ , K^+ , and Cl^-) act primarily by changing the Debye length, and their effect on surface potential can be accounted for within Guoy–Chapman theory. Divalent and higher-valent cations tend to adsorb to the surface, forming a Stern layer, which decreases the effective surface charge density. Changes in pH can also affect lipid headgroup ionization and, thus, the surface charge density. Lipid asymmetry induces local fields that affect ion channel function in neurons (5).

Surface potentials can also affect transmembrane ion transport by locally enhancing or depleting ion concentrations. For a -60 mV surface potential, the concentration of singly charged cationic species at the lipid–solution interface is approximately tenfold greater than in the bulk! This change in concentration can affect both the rate at which ions enter the pore of a transporter or channel and the rates at which small molecules or drugs bind to target receptors in the membrane.

Dipole potential. A second contribution to the voltage profile comes from the so-called dipole potential (17). This potential arises from oriented dipolar headgroups in zwitterionic lipids and cholesterol at the lipid–solution interface. To appreciate the origin of this potential, one can make an analogy to a parallel plate capacitor: In going from the negatively charged plate to the positively charged plate, there is clearly an increase in potential. Now, imagine creating the same charge distribution by lining up many dipoles in a plane, such that all of their plus ends form one charge sheet and their minus ends form another. Identical charge distributions must lead to identical potential profiles.

The dipole potential increases the electrostatic potential inside the membrane. This effect can be quite large: For example, phosphatidylcholine has a dipole potential of 220–280 mV (18). Cholesterol has been shown to increase the dipole potential and thereby to affect charge-transfer rates in the photosynthetic reaction center of *Rhodobacter sphaeroides* (67). Similar to the surface potential, asymmetry in the dipole potential can generate an intramembrane electric field. Thus, if one face of the membrane contains more dipolar species than the opposing face, there will be an electric field in the membrane even in the absence of a macroscopically measurable membrane potential.

Which parameter is correct—the local field or global potential? The answer depends on the process being studied. The equilibrium distribution of ions between the bulk phases depends only on the global potential difference. In contrast, conformational changes in transmembrane proteins depend on the local electric field. Interactions of soluble ions with transmembrane proteins are sensitive to the potential profile in the double layer and in the membrane. Thus, one should not anticipate perfect correspondence between optical and electrode-based voltage measurements. Indeed, differences between local field and global potential have been observed using organic voltage-sensitive dyes, and these differences may be a means by which neurons generate spatially varying thresholds for ion channel activation (5, 95). Internally generated membrane fields change slowly compared with the timescale of an action potential, making them difficult to detect with reporters of relative voltage. Reporters of absolute voltage promise to elucidate mechanisms by which cells regulate intramembrane electric fields.

THE FUTURE OF OPTICAL ELECTROPHYSIOLOGY

Although one can measure temperature and pH using physical electrodes, fluorescent molecular reporters are often more convenient (57, 97). Similarly, fluorescent molecular reporters facilitate noninvasive studies of membrane voltage in a dynamic cellular and organismal context. The

recent progress in the development of small-molecule and genetically encoded voltage reporters suggests that optical electrophysiology measurements will become routine in the near future.

Unfortunately, brighter, faster, more sensitive voltage indicators will not solve all of the challenges associated with optical electrophysiology. To accommodate the tremendous diversity of bioelectric phenomena, we must develop new classes of voltage indicators that contain novel molecular logic. Here, we illustrate three types of molecular logic that are needed.

Reporters of Absolute Voltage

Although most electrophysiology focuses on measuring rapid spikes in membrane voltage, slow shifts in baseline may be equally important. Baseline shifts are likely to regulate membrane transport and signaling and are hypothesized to be important in processes such as embryonic development (85) and wound healing (64), among others.

Reporters that convert membrane voltage directly into changes in fluorescence are good for detecting fast events such as action potentials. However, these reporters are less useful for measuring absolute numerical voltage values or for quantifying slow shifts in baseline voltage because the intensity measurements are confounded by photobleaching, background fluorescence, and variations in reporter concentration and illumination intensity. Patch clamp recordings can report absolute voltage during short-term measurements but are not sufficiently stable for long-term measurements. Dual-wavelength ratiometric measurements provide some ability to measure absolute voltage (5, 95, 101), but this approach requires careful calibration of the optical system and can be confounded by differential rates of photobleaching and by spectrally inhomogeneous background fluorescence.

A common strategy for obtaining accurate measurements is to translate a quantity such as voltage into the time domain. One could encode voltage information into a time-domain signal in several ways. For electrochromic organic voltage-sensitive dyes (58, 96), the lifetime of the electronic excited state likely depends on membrane voltage, allowing one- or two-photon fluorescence lifetime imaging (FLIM) to be a viable approach to absolute voltage measurements. A similar strategy might work for genetically encoded voltage indicators based on circularly permuted green fluorescent protein (GFP) (42). FLIM will work only if the voltage changes the quantum yield of the electronic excited state, however; this technique will not work if the voltage changes the ground-state absorption spectrum.

Rhodopsin-based voltage indicators offer an alternate strategy to measure absolute voltage. These proteins have a complex topology of optically and thermally driven transitions, several of which are sensitive to voltage. Thus, if one applies a stepwise change in illumination conditions (either in wavelength or intensity), the protein will relax to a new voltage- and illumination-dependent photostationary state, and in some Archaeorhodopsin mutants, e.g., Arch(D95H), the kinetics of this relaxation depend on membrane voltage. The population of the fluorescent state changes during this relaxation, so the dynamics of the transient fluorescence report the absolute membrane voltage. For many microbial rhodopsins, relaxation to a photostationary state occurs over tens to hundreds of milliseconds, so it can be monitored directly by wide-field imaging (39).

Voltage Integrators and Voltage Samplers

The invention of high-speed voltage indicators created an imaging problem: The moment an action potential finishes, the accompanying fluorescence signal disappears. Thus, unless one is looking at the neuron when it fires, one misses the event. As a mouse brain contains $\sim 7.5 \times 10^7$ neurons, there is no way to image all of them with sufficient temporal and spatial resolution to record their activity, even using the best voltage indicator conceivable. Neural recording

requires a data rate of at least 1 kHz. Whole-brain recording therefore requires a data rate of $\sim 10^{11}$ bytes/s, which is well beyond the capability of any imaging system. Furthermore, optical scattering prevents real-time optical access to brain regions deeper than ~ 1 mm below the surface.

An alternate strategy is to separate the encoding of the information from its readout. Suppose one could identify a photochemical reaction for which the reaction rate depended on the membrane voltage. Further suppose that the product was fluorescent and the starting material was not. One could then deliver a flash of diffuse light to the brain, perhaps paired with a stimulus. During the illumination epoch, the rate of photochemical product formation would be proportional to the local neural activity, allowing one to form a permanent photochemical imprint of activity. This imprint could be read out at a later time, either via slower scanning confocal imaging or by fixing the brain and slicing or clarifying the tissue. If one can identify a photochemically reversible reaction with the attributes described above, then one can repeat the process multiple times (provided the readout is not terminal).

Although the aforementioned molecular attributes may seem contrived, rhodopsin proteins can achieve this function (89). Many rhodopsins show optical bistability: The retinal in these moieties can be optically switched between different isomerization states that do not interconvert in the dark (35, 87). We have observed that optical interconversion rates in many rhodopsins are sensitive to voltage. Thus, naturally occurring or mildly mutated rhodopsins can serve as light-gated voltage integrators.

A variant on the integrator concept is a light-gated “sample-and-hold.” In some rhodopsins, light of a single wavelength can drive both a forward and reverse isomerization process. In the presence of light, there is a fast photostationary equilibrium between the isomerization states that can be voltage dependent. Thus, the protein may act as a conventional fast voltage indicator in the light. However, at the moment the illumination turns off, the distributions become fixed and can therefore be read out at a later time via fluorescence. Such a protein provides an instantaneous snapshot of neural activity at a moment in time.

One can think of these light-gated voltage reporters as providing a view of neural activity orthogonal to that of conventional patch clamp recordings. Patch clamp typically probes a single neuron for an extended time; in contrast, these photochemical techniques probe a large number of neurons—maybe even a complete brain—at a single moment.

CONCLUSION

In this review, we have sought to establish a conceptual framework for optical electrophysiology and to emphasize that electrophysiology and optogenetics are useful tools for everyone, not just neuroscientists. Decades of painstaking work by electrophysiologists and biophysicists have demonstrated a rich diversity of complex interactions of voltage, mechanical forces, ionic currents, and chemical reactions in biological systems. The advent of new optogenetic tools makes it tempting to start prospecting broadly for new bioelectric phenomena, and such prospecting will likely be highly productive. But, amid the bright lights of optical electrophysiology, one should remember that all bioelectric phenomena require careful quantitative analysis and that many fundamental physical mechanisms remain to be elucidated.

DISCLOSURE STATEMENT

Adam E. Cohen is a founder of Q-State Biosciences.

LITERATURE CITED

1. Accardi A, Miller C. 2004. Secondary active transport mediated by a prokaryotic homologue of ClC Cl-channels. *Nature* 427:803–7
2. Alford SC, Wu J, Zhao Y, Campbell RE, Knöpfel T. 2013. Optogenetic reporters. *Biol. Cell* 105:14–29
3. Bashford CL, Pasternak CA. 1986. Plasma membrane potential of some animal cells is generated by ion pumping, not by ion gradients. *Trends Biochem. Sci.* 11:113–16
4. Bass DA, Parce JW, Dechatelet LR, Szejda P, Seeds MC, Thomas M. 1983. Flow cytometric studies of oxidative product formation by neutrophils: a graded response to membrane stimulation. *J. Immunol.* 130:1910–17
5. Bedlack RS Jr, Wei MD, Fox SH, Gross E, Loew LM. 1994. Distinct electric potentials in soma and neurite membranes. *Neuron* 13:1187–93
6. Blaustein MP, Lederer WJ. 1999. Sodium/calcium exchange: its physiological implications. *Physiol. Rev.* 79:763–854
7. Booth IR. 2003. Bacterial ion channels. *Genet. Eng.* 25:91–111
8. Boyden ES, Zhang F, Bamberg E, Nagel G, Deisseroth K. 2005. Millisecond-timescale, genetically targeted optical control of neural activity. *Nat. Neurosci.* 8:1263–68
9. Bronner C, Mousli M, Eleno N, Landry Y. 1989. Resting plasma membrane potential of rat peritoneal mast cells is set predominantly by the sodium pump. *FEBS Lett.* 255:401–4
10. Brownell WE. 1990. Outer hair cell electromotility and otoacoustic emissions. *Ear Hear.* 11:82–92
11. Burton K, Wilson TH. 1953. The free-energy changes for the reduction of diphosphopyridine nucleotide and the dehydrogenation of L-malate and L-glycerol 1-phosphate. *Biochem. J.* 54:86–94
12. Cahalan MD, Chandy KG, DeCoursey TE, Gupta S. 1985. A voltage-gated potassium channel in human T lymphocytes. *J. Physiol.* 358:197–237
13. Cahalan MD, Wulff H, Chandy KG. 2001. Molecular properties and physiological roles of ion channels in the immune system. *J. Clin. Immunol.* 21:235–52
14. Cao G, Platasa J, Pieribone VA, Raccuglia D, Kunst M, Nitabach MN. 2013. Genetically targeted optical electrophysiology in intact neural circuits. *Cell* 154:904–13
15. Chanda B, Blunck R, Faria LC, Schweizer FE, Mody I, Bezanilla F. 2005. A hybrid approach to measuring electrical activity in genetically specified neurons. *Nat. Neurosci.* 8:1619–26
16. Chow BY, Han X, Dobry AS, Qian X, Chuong AS, et al. 2010. High-performance genetically targetable optical neural silencing by light-driven proton pumps. *Nature* 463:98–102
17. Clarke RJ. 2001. The dipole potential of phospholipid membranes and methods for its detection. *Adv. Colloid Interface Sci.* 89:263–81
18. Clarke RJ. 1997. Effect of lipid structure on the dipole potential of phosphatidylcholine bilayers. *Biochim. Biophys. Acta* 1327:269–78
19. Crane FL, Sun IL, Clark MG, Grebing C, Löw H. 1985. Transplasma-membrane redox systems in growth and development. *Biochim. Biophys. Acta* 811:233–64
20. DeCoursey TE, Morgan D, Cherny VV. 2003. The voltage dependence of NADPH oxidase reveals why phagocytes need proton channels. *Nature* 422:531–34
21. Delcour AH, Martinac B, Adler J, Kung C. 1989. Modified reconstitution method used in patch-clamp studies of *Escherichia coli* ion channels. *Biophys. J.* 56:631–36
22. Demchenko AP, Yesylevskyy SO. 2009. Nanoscopic description of biomembrane electrostatics: results of molecular dynamics simulations and fluorescence probing. *Chem. Phys. Lipids* 160:63–84
23. Felle H, Porter JS, Slayman CL, Kaback HR. 1980. Quantitative measurements of membrane potential in *Escherichia coli*. *Biochemistry* 19:3585–90
24. Fischer WB, Sansom MS. 2002. Viral ion channels: structure and function. *Biochim. Biophys. Acta* 1561:27–45
25. Frank HY, Yarov-Yarovoy V, Gutman GA, Catterall WA. 2005. Overview of molecular relationships in the voltage-gated ion channel superfamily. *Pharmacol. Rev.* 57:387–95
26. Freedman JC, Hoffman JF. 1979. The relation between dicarbocyanine dye fluorescence and the membrane potential of human red blood cells set at varying Donnan equilibria. *J. Gen. Physiol.* 74:187–212

27. Frizzell RA, Field M, Schultz SG. 1979. Sodium-coupled chloride transport by epithelial tissues. *Am. J. Physiol.* 236:F1–8
28. Gradinaru V, Thompson KR, Deisseroth K. 2008. eNpHR: a *Natronomonas* halorhodopsin enhanced for optogenetic applications. *Brain Cell Biol.* 36:129–39
29. Granier S, Kobilka B. 2012. A new era of GPCR structural and chemical biology. *Nat. Chem. Biol.* 8:670–73
30. Graves AR, Curran PK, Smith CL, Mindell JA. 2008. The Cl^-/H^+ antiporter ClC-7 is the primary chloride permeation pathway in lysosomes. *Nature* 453:788–92
31. Gray JP, Eisen T, Cline GW, Smith PJ, Heart E. 2011. Plasma membrane electron transport in pancreatic β -cells is mediated in part by NQO1. *Am. J. Physiol. Endocrinol. Metab.* 301:E113–21
32. Gustin MC, Martinac B, Saimi Y, Culbertson MR, Kung C. 1986. Ion channels in yeast. *Science* 233:1195–97
33. Haas M, Forbush B 3rd. 2000. The Na-K-Cl cotransporter of secretory epithelia. *Annu. Rev. Physiol.* 62:515–34
34. Hacking C, Eddy AA. 1981. The accumulation of amino acids by mouse ascites-tumour cells. Dependence on but lack of equilibrium with the sodium-ion electrochemical gradient. *Biochem. J.* 194:415–26
35. Hillebrecht JR, Koscielicki JF, Wise KJ, Marcy DL, Tetley W, et al. 2005. Optimization of protein-based volumetric optical memories and associative processors by using directed evolution. *NanoBiotechnology* 1:141–51
36. Hodgkin AL, Horowitz P. 1959. The influence of potassium and chloride ions on the membrane potential of single muscle fibres. *J. Physiol.* 148:127–60
37. Hoffman JF, Laris PC. 1974. Determination of membrane potentials in human and *Amphiuma* red blood cells by means of a fluorescent probe. *J. Physiol.* 239:519–52
38. Hörmann G. 1898. *Studien über die Protoplasmaströmung bei den Characeen*. Jena: Verlag von Gustav Fischer
39. Hou JH, Venkatachalam V, Cohen AE. 2014. Temporal dynamics of microbial rhodopsin fluorescence reports absolute membrane voltage. *Biophys. J.* 106:639–48
40. Iyer R, Iverson TM, Accardi A, Miller C. 2002. A biological role for prokaryotic ClC chloride channels. *Nature* 419:715–18
41. Jackson MB. 2006. *Molecular and Cellular Biophysics*. Cambridge, UK: Cambridge Univ. Press
42. Jin L, Han Z, Platasa J, Woollorton JRA, Cohen LB, Pieribone VA. 2012. Single action potentials and subthreshold electrical events imaged in neurons with a fluorescent protein voltage probe. *Neuron* 75:779–85
43. Kim GH, Kosterin P, Obaid AL, Salzberg BM. 2007. A mechanical spike accompanies the action potential in mammalian nerve terminals. *Biophys. J.* 92:3122–29
44. Kirichok Y, Krapivinsky G, Clapham DE. 2004. The mitochondrial calcium uniporter is a highly selective ion channel. *Nature* 427:360–64
45. Kirichok Y, Navarro B, Clapham DE. 2006. Whole-cell patch-clamp measurements of spermatozoa reveal an alkaline-activated Ca^{2+} channel. *Nature* 439:737–40
46. Kralj JM, Douglass AD, Hochbaum DR, Maclaurin D, Cohen AE. 2012. Optical recording of action potentials in mammalian neurons using a microbial rhodopsin. *Nat. Methods* 9:90–95
47. Kralj JM, Hochbaum DR, Douglass AD, Cohen AE. 2011. Electrical spiking in *Escherichia coli* probed with a fluorescent voltage-indicating protein. *Science* 333:345–48
48. Loewenstein WR, Kanno Y. 1963. Some electrical properties of a nuclear membrane examined with a microelectrode. *J. Gen. Physiol.* 46:1123–40
49. Maclaurin DM, Venkatachalam VV, Lee H, Cohen AE. 2013. Mechanism of voltage-sensitive fluorescence in a microbial rhodopsin. *Proc. Natl. Acad. Sci. USA* 110:5939–44
50. Maroudas A. 1968. Physicochemical properties of cartilage in the light of ion exchange theory. *Biophys. J.* 8:575–95
51. Martinac B, Buechner M, Delcour AH, Adler J, Kung C. 1987. Pressure-sensitive ion channel in *Escherichia coli*. *Proc. Natl. Acad. Sci. USA* 84:2297–301
52. Martinac B, Saimi Y, Kung C. 2008. Ion channels in microbes. *Physiol. Rev.* 88:1449–90

53. Mazzanti M, Bustamante JO, Oberleithner H. 2001. Electrical dimension of the nuclear envelope. *Physiol. Rev.* 81:1–19
54. McLaughlin S. 1989. The electrostatic properties of membranes. *Annu. Rev. Biophys. Biophys. Chem.* 18:113–36
55. McLaughlin S. 1977. Electrostatic potentials at membrane–solution interfaces. *Curr. Top. Membr. Transp.* 9:71–144
56. Metelkin E, Demin O, Kovács Z, Chinopoulos C. 2009. Modeling of ATP–ADP steady-state exchange rate mediated by the adenine nucleotide translocase in isolated mitochondria. *FEBS J.* 276:6942–55
57. Miesenböck G, De Angelis DA, Rothman JE. 1998. Visualizing secretion and synaptic transmission with pH-sensitive green fluorescent proteins. *Nature* 394:192–95
58. Miller EW, Lin JY, Frady EP, Steinbach PA, Kristan WB Jr, Tsien RY. 2012. Optically monitoring voltage in neurons by photo-induced electron transfer through molecular wires. *Proc. Natl. Acad. Sci. USA* 109:2114–19
59. Mitchell P. 1966. Chemiosmotic coupling in oxidative and photosynthetic phosphorylation. *Biol. Rev.* 41:445–502
60. Müller U, Malchow D, Hartung K. 1986. Single ion channels in the slime mold *Dictyostelium discoideum*. *Biochim. Biophys. Acta* 857:287–90
61. Murata Y, Iwasaki H, Sasaki M, Inaba K, Okamura Y. 2005. Phosphoinositide phosphatase activity coupled to an intrinsic voltage sensor. *Nature* 435:1239–43
62. Nicholls DG, Ferguson SJ, Ferguson S. 2002. *Bioenergetics*. Amsterdam: Academic. 3rd ed.
63. Nicholls DG, Ward MW. 2000. Mitochondrial membrane potential and neuronal glutamate excitotoxicity: mortality and millivolts. *Trends Neurosci.* 23:166–74
64. Nuccitelli R. 2003. A role for endogenous electric fields in wound healing. *Curr. Top. Dev. Biol.* 58:1–26
65. Peterka DS, Takahashi H, Yuste R. 2011. Imaging voltage in neurons. *Neuron* 69:9–21
66. Picollo A, Pusch M. 2005. Chloride/proton antiporter activity of mammalian CLC proteins CLC-4 and CLC-5. *Nature* 436:420–23
67. Pilotelle-Bunner A, Beaunier P, Tandori J, Maroti P, Clarke RJ, Sebban P. 2009. The local electric field within phospholipid membranes modulates the charge transfer reactions in reaction centres. *Biochim. Biophys. Acta* 1787:1039–49
68. Poburko D, Demaurex N. 2012. Regulation of the mitochondrial proton gradient by cytosolic Ca^{2+} signals. *Pflüg. Arch.* 464:19–26
69. Del Principe D, Avigliano L, Savini I, Catani MV. 2011. Trans–plasma membrane electron transport in mammals: functional significance in health and disease. *Antioxid. Redox Signal.* 14:2289–318
70. Raimondo JV, Kay L, Ellender TJ, Akerman CJ. 2012. Optogenetic silencing strategies differ in their effects on inhibitory synaptic transmission. *Nat. Neurosci.* 15:1102–4
71. Roos D, van Bruggen R, Meischl C. 2003. Oxidative killing of microbes by neutrophils. *Microb. Infect.* 5:1307–15
72. Rubinstein B, Luster DG. 1993. Plasma membrane redox activity: components and role in plant processes. *Annu. Rev. Plant Biol.* 44:131–55
73. Saddler HD. 1970. The membrane potential of *Acetabularia mediterranea*. *J. Gen. Physiol.* 55:802–21
74. Sanders D, Hansen UP, Slayman CL. 1981. Role of the plasma membrane proton pump in pH regulation in non-animal cells. *Proc. Natl. Acad. Sci. USA* 78:5903–7
75. Sanderson JB. 1872. Note on the electrical phenomena which accompany irritation of the leaf of *Dionaea muscipula*. *Proc. R. Soc. Lond.* 21:495–96
76. Schmid A, Dehlinger-Kremer M, Schulz I, Gögelein H. 1990. Voltage-dependent InsP3-insensitive calcium channels in membranes of pancreatic endoplasmic reticulum vesicles. *Nature* 346:374–76
77. Schrenzel J, Serrander L, Bánfi B, Nüße O, Fouyouzi R, et al. 1998. Electron currents generated by the human phagocyte NADPH oxidase. *Nature* 392:734–37
78. Schwenke WD, Soboll S, Seitz HJ, Sies H. 1981. Mitochondrial and cytosolic ATP/ADP ratios in rat liver in vivo. *Biochem. J.* 200:405–8
79. Slayman CL. 1965. Electrical properties of *Neurospora crassa*. Respiration and the intracellular potential. *J. Gen. Physiol.* 49:93–116

80. Spanswick RM. 1981. Electrogenic ion pumps. *Annu. Rev. Plant Physiol.* 32:267–89
81. Srivastava M, Duong LT, Fleming PJ. 1984. Cytochrome b561 catalyzes transmembrane electron transfer. *J. Biol. Chem.* 259:8072–75
82. Stappen R, Krämer R. 1993. Functional properties of the reconstituted phosphate carrier from bovine heart mitochondria: evidence for asymmetric orientation and characterization of three different transport modes. *Biochim. Biophys. Acta* 1149:40–48
83. Sulavik MC, Houseweart C, Cramer C, Jiwani N, Murgolo N, et al. 2001. Antibiotic susceptibility profiles of *Escherichia coli* strains lacking multidrug efflux pump genes. *Antimicrob. Agents Chemother.* 45:1126–36
84. Sun IL, Sun EE, Crane FL, Morré DJ, Lindgren A, Löw H. 1992. Requirement for coenzyme Q in plasma membrane electron transport. *Proc. Natl. Acad. Sci. USA* 89:11126–30
85. Sundelacruz S, Levin M, Kaplan DL. 2009. Role of membrane potential in the regulation of cell proliferation and differentiation. *Stem Cell Rev.* 5:231–46
86. Taglicht D, Padan E, Schuldiner S. 1993. Proton-sodium stoichiometry of NhaA, an electrogenic antiporter from *Escherichia coli*. *J. Biol. Chem.* 268:5382–87
87. Tsukamoto H, Terakita A. 2010. Diversity and functional properties of bistable pigments. *Photochem. Photobiol. Sci.* 9:1435–43
88. van der Schoot P, Bruinsma R. 2005. Electrostatics and the assembly of an RNA virus. *Phys. Rev. E* 71:061928
89. Venkatachalam V, Brinks D, Maclaurin D, Hochbaum D, Kralj J, Cohen AE. 2014. Flash memory: photochemical imprinting of neuronal action potentials onto a microbial rhodopsin. *J. Am. Chem. Soc.* 136:2529–37
90. Villalba JM, Navarro F, Córdoba F, Serrano A, Arroyo A, et al. 1995. Coenzyme Q reductase from liver plasma membrane: purification and role in trans-plasma-membrane electron transport. *Proc. Natl. Acad. Sci. USA* 92:4887–91
91. Volkov AG, ed. 2006. *Plant Electrophysiology: Theory and Methods*. Berlin: Springer
92. Winterhalter M, Helfrich W. 1992. Bending elasticity of electrically charged bilayers: coupled monolayers, neutral surfaces, and balancing stresses. *J. Phys. Chem.* 96:327–30
93. Winterhalter M, Helfrich W. 1988. Effect of surface charge on the curvature elasticity of membranes. *J. Phys. Chem.* 92:6865–67
94. Wood PM. 1974. The redox potential of the system oxygen—superoxide. *FEBS Lett.* 44:22–24
95. Xu C, Loew LM. 2003. The effect of asymmetric surface potentials on the intramembrane electric field measured with voltage-sensitive dyes. *Biophys. J.* 84:2768–80
96. Yan P, Acker CD, Zhou W, Lee P, Bollensdorff C, et al. 2012. Palette of fluorinated voltage-sensitive hemicyanine dyes. *Proc. Natl. Acad. Sci. USA* 109:20443–48
97. Yang J-M, Yang H, Lin L. 2011. Quantum dot nano thermometers reveal heterogeneous local thermogenesis in living cells. *ACS Nano* 5:5067–71
98. Yao H, Haddad GG. 2004. Calcium and pH homeostasis in neurons during hypoxia and ischemia. *Cell Calcium* 36:247–55
99. Zhang C, Xiong W, Zheng H, Wang L, Lu B, Zhou Z. 2004. Calcium- and dynamin-independent endocytosis in dorsal root ganglion neurons. *Neuron* 42:225–36
100. Zhang C, Zhou Z. 2002. Ca²⁺-independent but voltage-dependent secretion in mammalian dorsal root ganglion neurons. *Nat. Neurosci.* 5:425–30
101. Zhang J, Davidson RM, Wei MD, Loew LM. 1998. Membrane electric properties by combined patch clamp and fluorescence ratio imaging in single neurons. *Biophys. J.* 74:48–53